

# Ultra Low Overhead Syndrome Extraction for the Steane code

Boldizsár Poór,<sup>1,2</sup> Benjamin Rodatz,<sup>1,2</sup> and Aleks Kissinger<sup>1</sup>

<sup>1</sup>*University of Oxford, United Kingdom*

<sup>2</sup>*Quantinuum, United Kingdom*

We establish a new performance benchmark for the fault-tolerant syndrome extraction of  $[[7, 1, 3]]$  Steane code with a dynamic protocol. Our method is built on two highly optimized circuits derived using fault-equivalent ZX-rewrites: a primary fault-tolerant circuit with 14 CNOTs and an efficient non-fault-tolerant recovery circuit with 11 CNOTs. The protocol uses an adaptive response to internal faults, discarding flagged measurements and falling back to the recovery circuit to correct potentially detrimental errors. Monte Carlo simulations confirm the efficiency of our protocol, reducing the logical error rate per cycle by an average of  $\sim 14.3\%$  relative to the optimized Steane method [1] and  $\sim 17.7\%$  compared to the Reichardt's three-qubit method [2], the leading prior techniques.

## I. INTRODUCTION

The realization of a scalable quantum computer heavily relies on the implementation of fault-tolerant quantum error correction to protect quantum information from environmental noise. In particular, one of the most ubiquitously used gadgets when aiming to realize fault-tolerant quantum computing (FTQC) is the syndrome measurement circuit. Not only is it used to measure syndromes and correct errors regularly [1], but it is also essential for many magic state preparation schemes [3–5]. It is therefore crucial that the implementation of this gadget is fault-tolerant and introduces minimal additional noise.

Within the vast space of quantum error correction (QEC) codes, the  $[[7, 1, 3]]$  Steane code is one of the most fundamental and well-studied examples. Discovered by Andrew Steane in 1996 [6], it is a self-dual CSS code constructed from the classical  $[7, 4, 3]$  Hamming code, and is the smallest CSS code capable of correcting a single-qubit error [7]. As a CSS code, its X and Z syndromes can be extracted independently, making low overhead Steane-style syndrome extraction possible [8]. The recursive concatenation of the Steane code yields one of the first code families proven to admit a concatenated threshold [9]. Due to these important theoretical properties and its small size, it remains one of the most experimentally realized QEC codes to date [10–13].

Beyond the generally applicable methods proposed by Shor [1] and Steane [8], several fault-tolerant (FT) syndrome extraction (SE) schemes have been developed for the Steane code. For low overhead, the dominant strategy has been the dynamic ‘flag-and-fallback’ approach. Examples of this approach include the *two-qubit* method proposed by Chao and Reichardt [14], later improved by Bhatnagar *et al.* [15], and the *three-qubit* method by Reichardt [2]. This approach works by continuously measuring syndromes with a flagged circuit that can detect internal faults. If a flag is raised, the protocol switches to a simpler, non-fault-tolerant (non-FT) ‘recovery’ SE circuit that diagnoses the most likely fault. While the protocol includes a non-FT component, the full protocol is fault-tolerant according to the extended rectangle

formalism for distance-three codes [14, 16].

Recently, Rodatz *et al.* [17] introduced a novel static SE circuit which, while not universally optimal, achieves state-of-the-art performance in many important contexts. The circuit was derived using the ZX-calculus [18] — a graphical language for representing and reasoning about quantum computation. This was achieved by constructing a Steane-style SE circuit with the fault-tolerant state preparation circuit of Goto [19], and then reducing gate and qubit count using fault-equivalent rewrites [17, 20]. While this static approach results in a highly efficient circuit, it can leave the logical state corrupted between syndrome measurements.

This work builds on the rewrite-based approach of Rodatz *et al.* [17], introducing two key improvements. First, by employing a more exhaustive application of fault-equivalent rewrites, combined with further code-level observations, we derive two highly optimized SE circuits: a primary fault-tolerant version with 14 CNOTs and 4 ancillae, and a leaner non-FT ‘recovery’ circuit with 11 CNOTs and 3 ancillae. Both of these circuits use provably optimal number of CNOT gates in their particular settings. Second, we introduce an adaptive fallback mechanism for when a flag is raised. This dynamic mechanism introduces minimal overhead because — unlike previous methods [2, 14] — our primary circuit can correct non-trivial syndromes on its own, and falling back to the recovery circuit is only necessary upon the measurement of a raised flag. Monte Carlo simulations under a realistic near-term hardware noise model demonstrate the high efficiency of our protocol. It reduces the logical error rate per cycle by an average of  $\sim 14.3\%$  against the optimized Steane [17] and by  $\sim 17.7\%$  against the three-qubit method [2].

## II. CIRCUITS AND DYNAMIC PROTOCOL

In this section, we introduce the two circuits that form the core of our new protocol and detail the dynamic procedure that uses them. The first is a fault-tolerant syndrome extraction circuit optimized for low overhead,

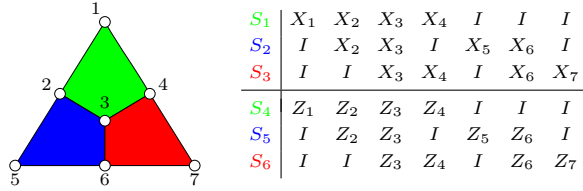


FIG. 1: Qubit layout and stabilizer structure of the Steane code, as given in [10].

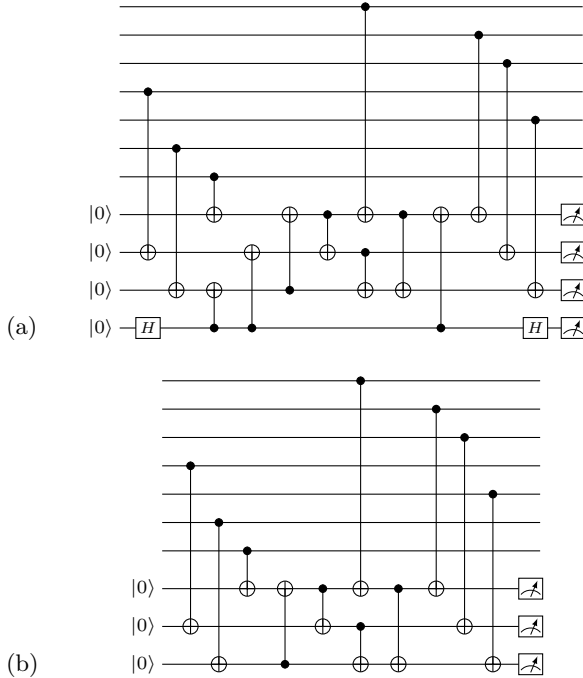


FIG. 2: Optimized syndrome extraction circuits for of our dynamic protocol: (a) fault-tolerant primary circuit using 14 CNOTs and 4 ancillae, and (b) non-fault-tolerant recovery circuit using 11 CNOTs and 3 ancillae. The Steane code’s self-duality yields structurally identical X-syndrome measurements.

while the second is an even leaner non-fault-tolerant ‘recovery’ circuit. Figure 2 shows the final form of our circuits for measuring the Z stabilizers of the Steane code.

To derive these circuits, we start from the same circuit as in previous works [17]: the Steane-style syndrome extraction circuit with Goto’s probabilistic state preparation [19] (adopted to the qubit layout shown in Figure 1). Then, to reduce gate and qubit count, we apply fault-equivalent rewrites — ZX manipulations that provably preserve a circuit’s behaviour under noise, and thus, its tolerance to faults [17, 20]. The non-FT version has its flag qubit removed to minimize overhead. The full derivations are detailed in Appendix A.

In Appendix B, we examine the optimality of the cir-

cuits’ CNOT count and find that for the non-FT setting, 11 CNOTs are minimal; furthermore, given an 11 CNOT circuit, at least 3 CNOTs are necessary to flag (on a separate qubit) any ‘problematic’ internal fault.

### A. Decoding Logic

The optimized nature of these circuits leads to a slightly more involved decoding procedure, which we detail here. The overall goal is to correctly infer the required correction on data qubits while accounting for possible internal faults within the SE circuit itself.

#### 1. No Flag Raised

In the ideal case where the flag qubit outcome is 0 during the primary circuit’s execution, no internal fault is detected. The process to identify the data-error begins with the raw measurement outcome, a 3-bit string  $b$  obtained from the three ancillae. This raw outcome, however, is not the syndrome itself. To convert it into the standard syndrome of the Steane code, it must be transformed by the circuit’s effective parity-check matrix<sup>1</sup>:

$$H'_x = H'_z = \begin{pmatrix} 1 & 1 & 0 \\ 1 & 1 & 1 \\ 0 & 1 & 0 \end{pmatrix} \quad (1)$$

The result of the multiplication,  $s := H'_x \cdot b$ , is the true 3-bit syndrome. With the syndrome calculated, the location of the error is found by matching  $s$  to the corresponding column of the full parity-check matrix:

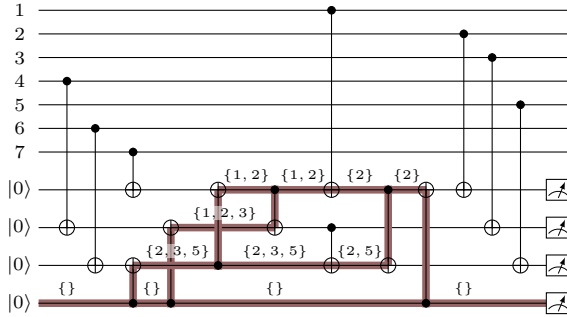
$$H_x = H_z = \begin{pmatrix} 1 & 1 & 1 & 1 & 0 & 0 & 0 \\ 0 & 1 & 1 & 0 & 1 & 1 & 0 \\ 0 & 0 & 1 & 1 & 0 & 1 & 1 \end{pmatrix} \quad (2)$$

For instance, if the raw measurement is  $b = (0, 1, 1)^T$ , the calculated syndrome becomes  $s = H'_x \cdot b = (1, 0, 1)^T$ . This syndrome matches the 4th column of  $H_x$ , indicating that a correction should be applied to the 4th data qubit.

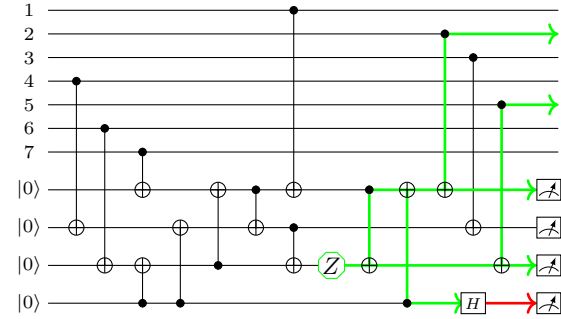
#### 2. Flag Raised

A flag measurement outcome of 1 indicates an internal fault in the primary SE circuit. Such a fault can propagate to the data qubits, resulting in a multi-qubit error (Figure 3b), which would not be corrected by the standard decoder. In order to correctly fix any potential error, we modify the decoding logic for the subsequent measurement of the opposite syndrome.

<sup>1</sup>This matrix is derived from the parity-check matrix of Eq. (2) by keeping only columns 2, 3, and 5, as detailed in Theorem 1.



(a) The detecting region of the FT circuit. A fault on a highlighted edge is caught by the flag qubit. Each location label corresponds to its resulting data-qubit error.



(b) An example of fault propagation. A single ancilla fault creates a weight-two error on the data qubits.

FIG. 3: Circuit with (a) flagged errors and (b) an example of how an error spreads.

Labels in Figure 3a mark space-time locations, each label identifying how the given error would spread to the data qubits. Some of these errors are correctable by the standard decoder; for instance, the error  $\{2, 3, 5\}$  propagates to the weight-three error  $Z_2 Z_3 Z_5$ , which is stabilizer-equivalent to the single-qubit error  $Z_6$ , and is therefore handled correctly by the standard decoder. However, other faults are problematic, as they correspond to weight-two data-qubit errors (e.g.  $\{2, 5\}$  shown in Figure 3b), which the standard decoder would misidentify and introduce a logical error ( $Z_2 Z_5 \sim Z_1 \bar{Z}$ ).

To correctly fix all flagged faults, the decoding logic is modified for errors  $\{1, 2\}$  and  $\{2, 5\}$ . Respectively, these faults result in  $Z_1 Z_2$  and  $Z_2 Z_5$  on the data, which produce syndromes  $(0, 1, 0)^T$  and  $(1, 0, 0)^T$ . These syndromes would normally indicate a correction on the fifth and the first qubit, which we modify to instead correct qubits 1 & 2, and qubits 2 & 5, respectively. All other syndromes continue to map to their standard single-qubit corrections. Assuming only a single fault occurs, this dynamic remapping allows for an unambiguous correction.

## B. Protocol Operation

The operational flow of our dynamic protocol is summarized in the flowchart in Figure 4. A cycle begins with the execution of the primary FT circuit (Figure 2a). If the flag qubit measurement outcome is 0, the results are decoded using the standard procedure detailed in Section II A 1. If the flag outcome is 1, the measurement outputs from the primary SE gadget are discarded. The protocol then executes the non-FT ‘recovery’ circuit (Figure 2b) in the dual basis, and the measurement outcomes from this recovery run are decoded using the modified logic described in Section II A 2.

While the recovery circuit is not fault-tolerant on its own, we still obtain a protocol that is fault-tolerant according to the extended rectangle formalism for distance-three codes [16, 21], following a similar argument to [14, Page 2]. In particular,

- (i) if there is at most a single data error before measurement and no internal fault occurs, it appropriately corrects the error;
- (ii) if the data lies in the codespace and at most one internal fault occurs in the primary circuit, then
  - (a) if the flag is not raised, at most a weight-one error propagates to the data.
  - (b) if a flag is raised, then the subsequent recovery circuit suffices to correct any possible error, assuming that no additional errors take place.

## III. SIMULATIONS

To validate the performance of our protocol, we conducted Monte Carlo simulations using Stim [22]. We compare our syndrome extraction protocol with the following methods:

- The three-qubit method [2], as the most established and experimentally demonstrated method.
- Steane-style syndrome extraction [8] with Goto’s state preparation [19], as the basis of this work.
- Optimized Steane-style syndrome extraction [17], the direct predecessor of this work.

*a. Noise model* We assume circuit-level depolarizing noise with error probabilities  $p_2$  for two-qubit gates,  $p_{\text{SPAM}}$  for (only) measurement, and  $p_{\text{mem}}$  for idle qubits. A  $Z$ -type memory error is applied to all idling qubits, and non-interacting gates are assumed to execute in parallel. We set  $p_2 = p_{\text{SPAM}} = p_{\text{phys}}$  and  $p_{\text{mem}} = 0.1 p_{\text{phys}}$ .

*b. Results* In the first set of simulations, we vary the physical error rate  $p_{\text{phys}}$  and compute the corresponding logical error probability  $p_L$  per correction cycle. Our method achieves a consistently lower logical error probability than previous approaches; see Figure 5. The number of samples for each data point is scaled inversely with

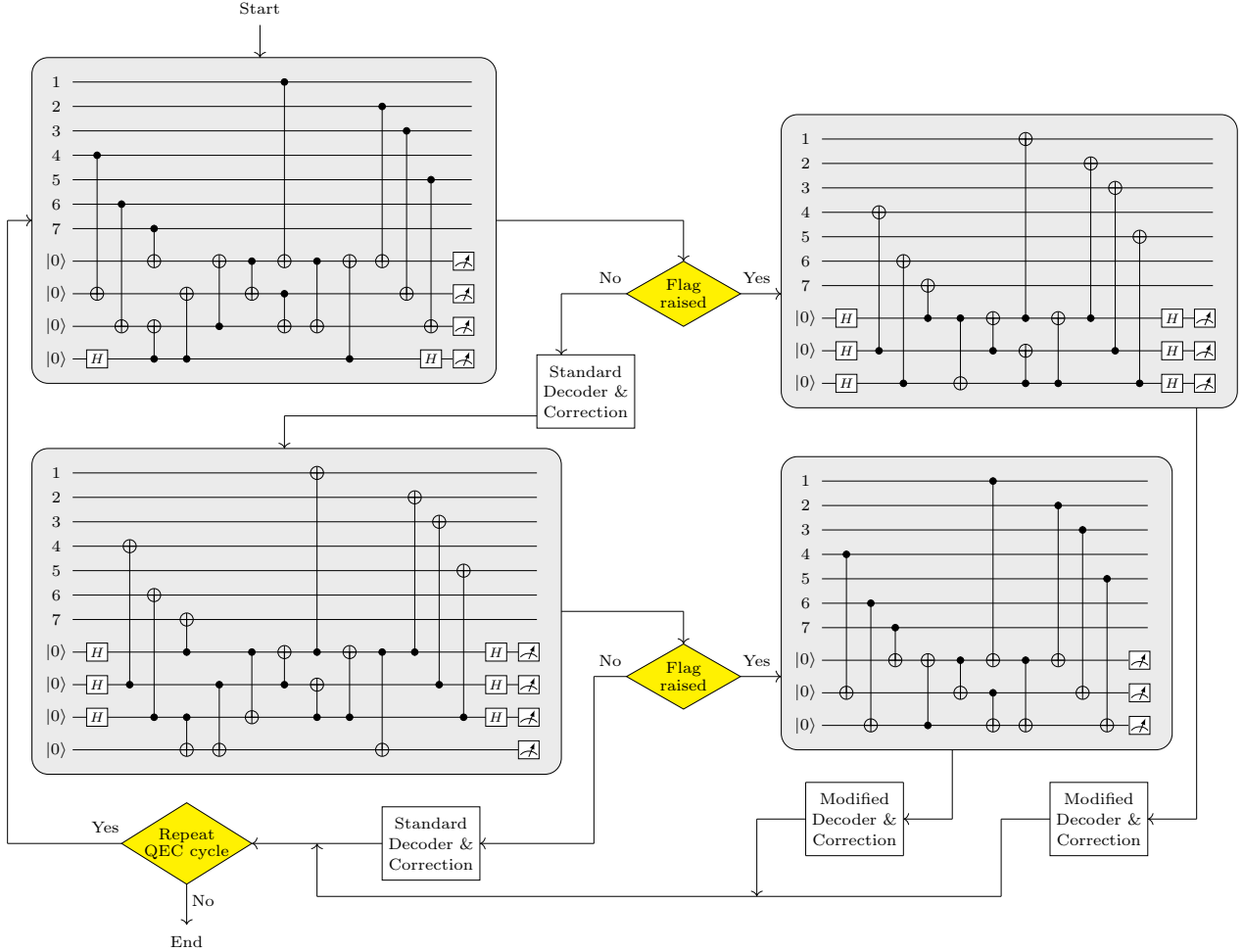


FIG. 4: Flowchart of the full syndrome extraction protocol for a single cycle.

$p_{\text{phys}}$ , taking  $20,000/p_{\text{phys}}$  samples to ensure statistical significance.

In a second simulation, we evaluate performance under a realistic near-term hardware noise model with fixed parameters  $p_2 = p_{\text{SPAM}} = 10^{-3}$  and  $p_{\text{mem}} = 10^{-4}$ . We repeat the syndrome measurement and correction cycles and observe that our method consistently maintains the lowest logical error rates (Figure 6). Each data point is averaged over 10,000,000 samples.

Table I summarizes the average decrease of logical error probability per data point compared to the other approaches for both experiments.

#### IV. SUMMARY AND OUTLOOK

This paper introduces an adaptive, ultra low overhead fault-tolerant syndrome extraction protocol for the Steane code. The protocol uses two highly optimized circuits derived using fault-equivalent ZX rewrites, a fault-tolerant and a non-fault-tolerant SE circuit with provably

	vs. Steane	vs. Opt. Steane	vs. 3-qubit
Decrease of $\frac{p_L}{p_{\text{phys}}}$	$Z$ basis	9.4%	6.2%
	$X$ basis	18.1%	12.0%
	Average	15.2%	10.0%
Decrease of $\frac{p_L}{N}$	$Z$ basis	26.8%	14.6%
	$X$ basis	25.0%	14.1%
	Average	25.5%	14.3%

TABLE I: Average decrease (%) in logical error probability of our method relative to prior approaches.

optimal CNOT counts in their respective settings. Together, these circuits form a dynamic ‘flag-and-fallback’ protocol that corrects both data errors and internal faults with minimal overhead. Achieving further optimization for a code as extensively studied as the Steane code highlights that even small, well-understood codes offer room for improvement, and that combining fault-equivalent

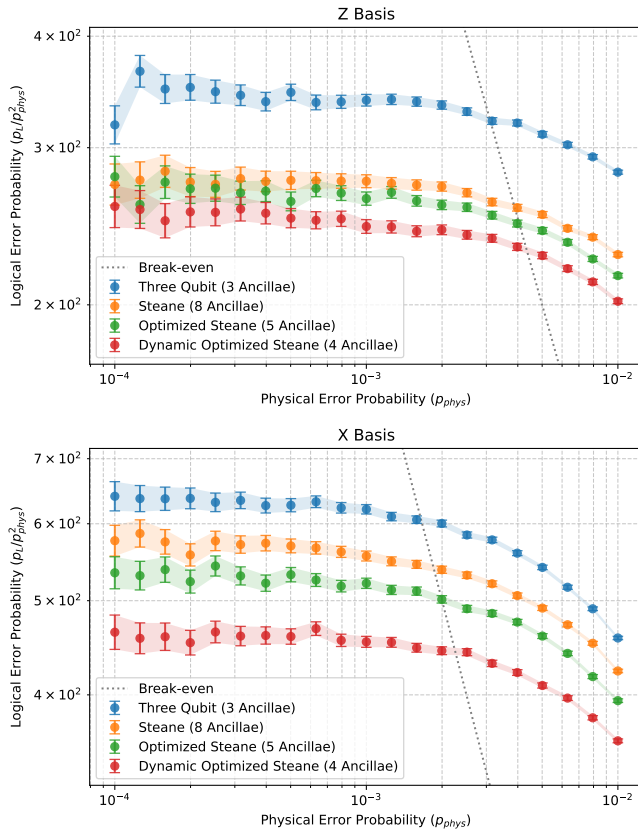


FIG. 5: Logical error rate  $p_L/p_{\text{phys}}^2$  as a function of physical error rate  $p_{\text{phys}}$ , with Wilson confidence intervals.

rewrites with code-level insights can help us discover new highly efficient methods.

The present protocol provides a practical template for distance-three codes. The process begins with optimizing a Steane-style syndrome extraction circuit using fault-equivalent rewrites. As long as flagged internal faults result in unique syndromes, the same dynamic strategy applies directly to other distance-three codes. Two main challenges remain in generalizing this approach. For larger SE gadgets, the optimization process becomes more complex with increased circuit depth with current techniques. This motivates the development of systematic, automated methods for fault-tolerant circuit optimization, potentially involving new classes of fault-equivalent rewrites. The second challenge concerns the dynamic aspect itself: for higher-distance codes, switching from FT to non-FT circuits would not satisfy Gottesman's criteria for fault tolerance. Extending the approach to this regime will require a dynamic mechanism with intermediate steps to preserve full fault tolerance.

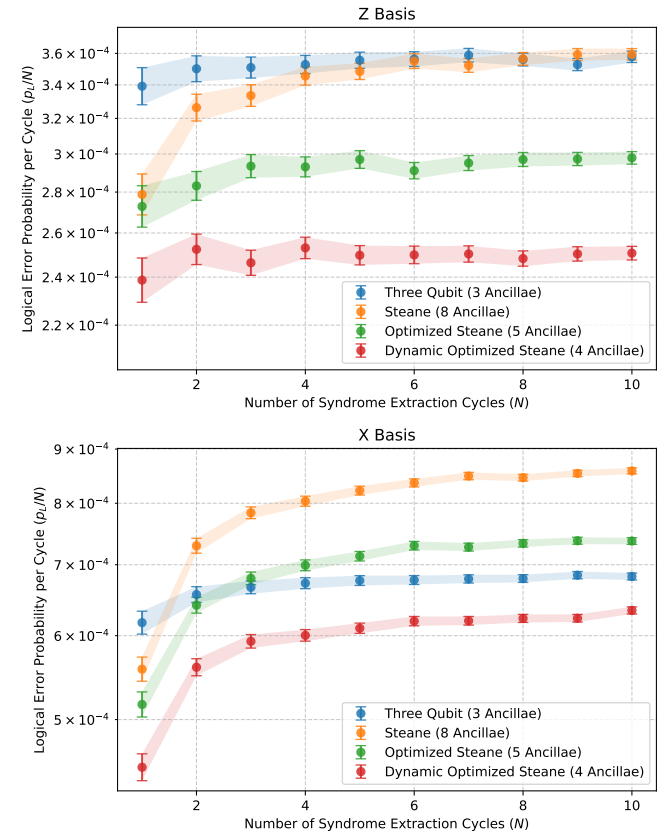


FIG. 6: Logical error rate per cycles  $p_L/N$  as a function of the number of error correction cycles  $N$ , with Wilson confidence intervals.

## DATA AVAILABILITY

The simulation files, numerical data, and the processing scripts necessary to reproduce the figures in this work are available at [23].

## ACKNOWLEDGMENTS

We thank Andrey Boris Khesin and Razin A. Shaikh for discussions on optimality of CNOT counts. We appreciate the helpful reviews and numerous suggestions for improvement from David Amaro and Selwyn Simsek. BP and AK are supported by the Engineering and Physical Sciences Research Council grant number EP/Z002230/1, “(De)constructing quantum software (DeQS)”. BR thanks Simon Harrison for his generous support for the Wolfson Harrison UK Research Council Quantum Foundation Scholarship. The authors used automated language tools for editorial assistance.

[1] P. Shor, in *Proceedings of 37th Conference on Foundations of Computer Science* (1996) pp. 56–65.

[2] B. W. Reichardt, *Quantum Science and Technology* **6**, 015007 (2020).

[3] S. B. Bravyi and A. Y. Kitaev, Quantum codes on a lattice with boundary (1998), arXiv:quant-ph/9811052.

[4] C. Chamberland and K. Noh, *npj Quantum Information* **6**, 91 (2020).

[5] C. Gidney, N. Shutty, and C. Jones, Magic state cultivation: Growing T states as cheap as CNOT gates (2024), arXiv:2409.17595.

[6] A. Steane, *Proceedings of the Royal Society of London. Series A: Mathematical, Physical and Engineering Sciences* **452**, 2551 (1997), arXiv:quant-ph/9601029.

[7] B. Shaw, M. M. Wilde, O. Oreshkov, I. Kremsky, and D. A. Lidar, *Physical Review A* **78**, 012337 (2008).

[8] A. M. Steane, *Physical Review Letters* **78**, 2252 (1997).

[9] E. Knill, R. Laflamme, and W. H. Zurek, *Proceedings of the Royal Society of London. Series A: Mathematical, Physical and Engineering Sciences* **454**, 365 (1998).

[10] C. Ryan-Anderson, J. G. Bohnet, K. Lee, D. Gresh, A. Hankin, J. P. Gaebler, D. Francois, A. Chernoguzov, D. Lucchetti, N. C. Brown, T. M. Gatterman, S. K. Halit, K. Gilmore, J. A. Gerber, B. Neyenhuis, D. Hayes, and R. P. Stutz, *Physical Review X* **11**, 041058 (2021).

[11] A. Paetznick, M. P. da Silva, C. Ryan-Anderson, J. M. Bello-Rivas, J. P. C. III, A. Chernoguzov, J. M. Dreiling, C. Foltz, F. Frachon, J. P. Gaebler, T. M. Gatterman, L. Grans-Samuelsson, D. Gresh, D. Hayes, N. Hewitt, C. Holliman, C. V. Horst, J. Johansen, D. Lucchetti, Y. Matsuoka, M. Mills, S. A. Moses, B. Neyenhuis, A. Paz, J. Pino, P. Siegfried, A. Sundaram, D. Tom, S. J. Wernli, M. Zanner, R. P. Stutz, and K. M. Svore, Demonstration of logical qubits and repeated error correction with better-than-physical error rates (2024), arXiv:2404.02280.

[12] D. Bluvstein, S. J. Evered, A. A. Geim, S. H. Li, H. Zhou, T. Manovitz, S. Ebadi, M. Cain, M. Kalinowski, D. Hangleiter, J. P. Bonilla Ataides, N. Maskara, I. Cong, X. Gao, P. Sales Rodriguez, T. Karolyshyn, G. Semeghini, M. J. Gullans, M. Greiner, V. Vuletić, and M. D. Lukin, *Nature* **626**, 58 (2024).

[13] L. Postler, F. Butt, I. Pogorelov, C. D. Marciniak, S. Heußen, R. Blatt, P. Schindler, M. Rispler, M. Müller, and T. Monz, *PRX Quantum* **5**, 030326 (2024).

[14] R. Chao and B. W. Reichardt, *Physical Review Letters* **121**, 050502 (2018).

[15] D. Bhatnagar, M. Steinberg, D. Elkouss, C. G. Almudever, and S. Feld, in *2023 IEEE International Conference on Quantum Computing and Engineering (QCE)*, Vol. 01 (2023) pp. 63–69.

[16] P. Aliferis, D. Gottesman, and J. Preskill, *Quantum Information and Computation* **6**, 97 (2006), arXiv:quant-ph/0504218.

[17] B. Rodatz, B. Poór, and A. Kissinger, Fault Tolerance by Construction (2025), arXiv:2506.17181.

[18] B. Coecke and R. Duncan, in *Automata, Languages and Programming*, Lecture Notes in Computer Science, edited by L. Aceto, I. Damgård, L. A. Goldberg, M. M. Halldórsson, A. Ingólfssdóttir, and I. Walukiewicz (Springer, Berlin, Heidelberg, 2008) pp. 298–310.

[19] H. Goto, *Scientific Reports* **6**, 19578 (2016).

[20] B. Rodatz, B. Poór, and A. Kissinger, Floquetifying stabiliser codes with distance-preserving rewrites (2024), arXiv:2410.17240.

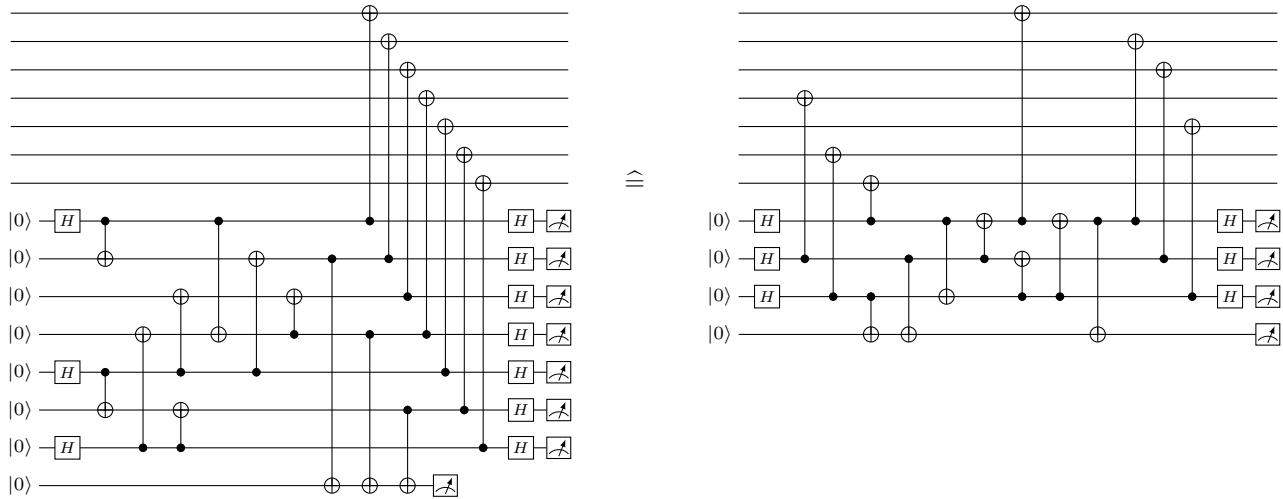
[21] D. Gottesman, *Surviving as a Quantum Computer in a Classical World* (2024).

[22] C. Gidney, *Quantum* **5**, 497 (2021).

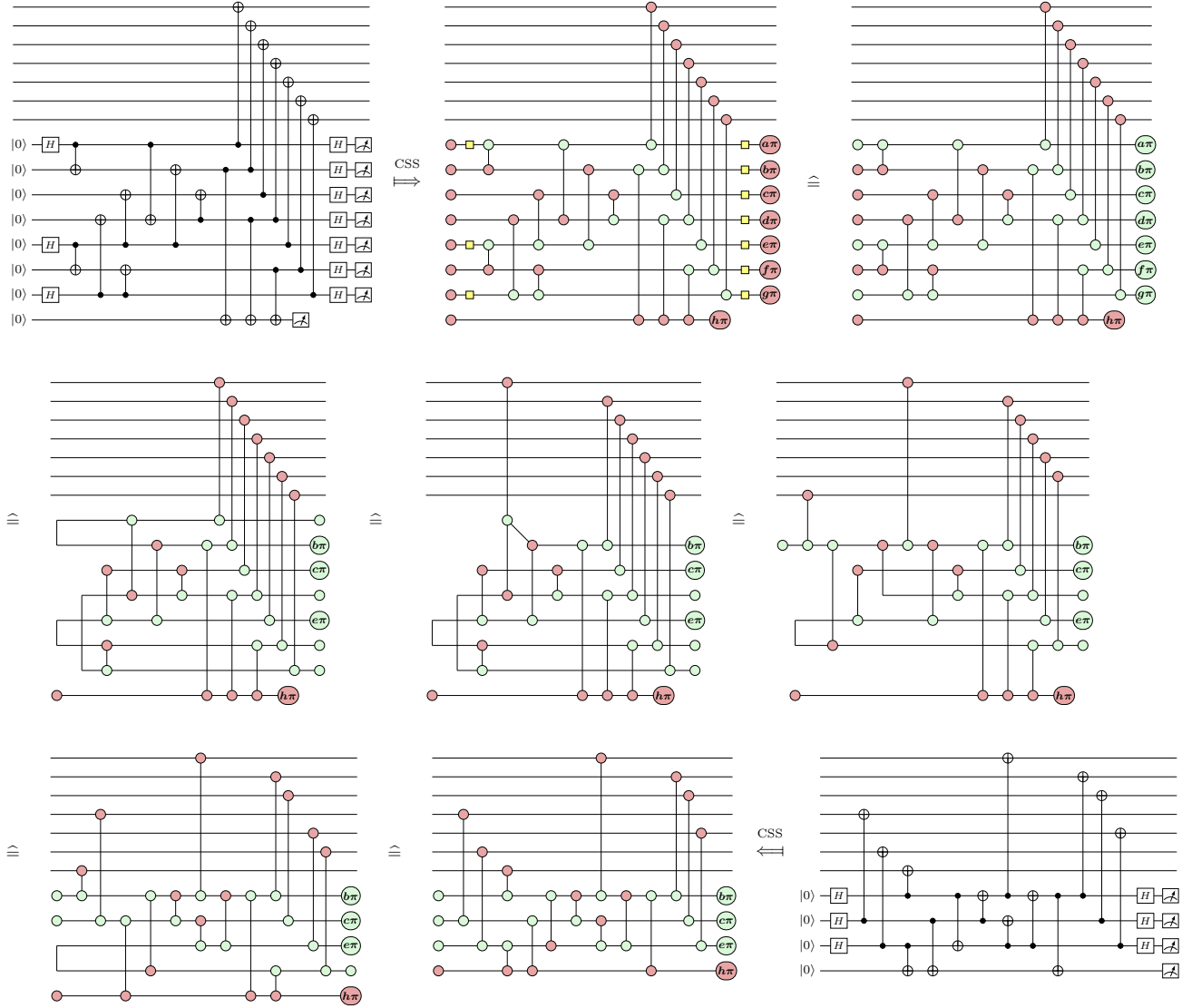
[23] boldar99/Steane-Ultra-Low-Overhead.

## Appendix A: Derivations

**Theorem 1.** The following transformation is fault-equivalent:



*Proof.* The fault-equivalence of such a mapping is established for CSS codes in [17, Section 7].



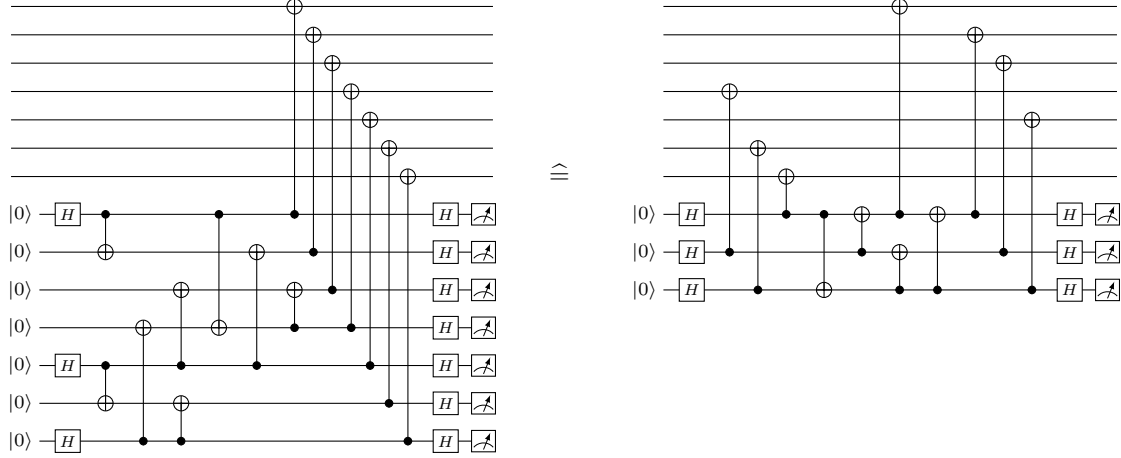
The proof uses several ZX rewrite rules, including Color Change, Fusion, Identity, and the OCM (Only Connected Measurements) rule. The fault-equivalence of these rewrites is proven in [17, 20].

A key step, marked by (\*) in the proof, involves setting the phase of certain measurement spiders to zero, which is equivalent to post-selecting on their measurement outcomes. However, because these spiders are not extracted as measurements in the final diagram, the process yields a physically realizable and fully deterministic quantum circuit with no post-selection and fewer ancillae. Despite this reduction, the full syndrome  $s$  can still be recovered using an effective parity-check matrix,  $H'_x$ , which is formed by keeping only the columns of the original matrix  $H_x$  that correspond to the remaining measurements (in this case, columns 2, 3, and 5). We can verify that no syndrome information is lost, since the effective and full matrices have the same rank:

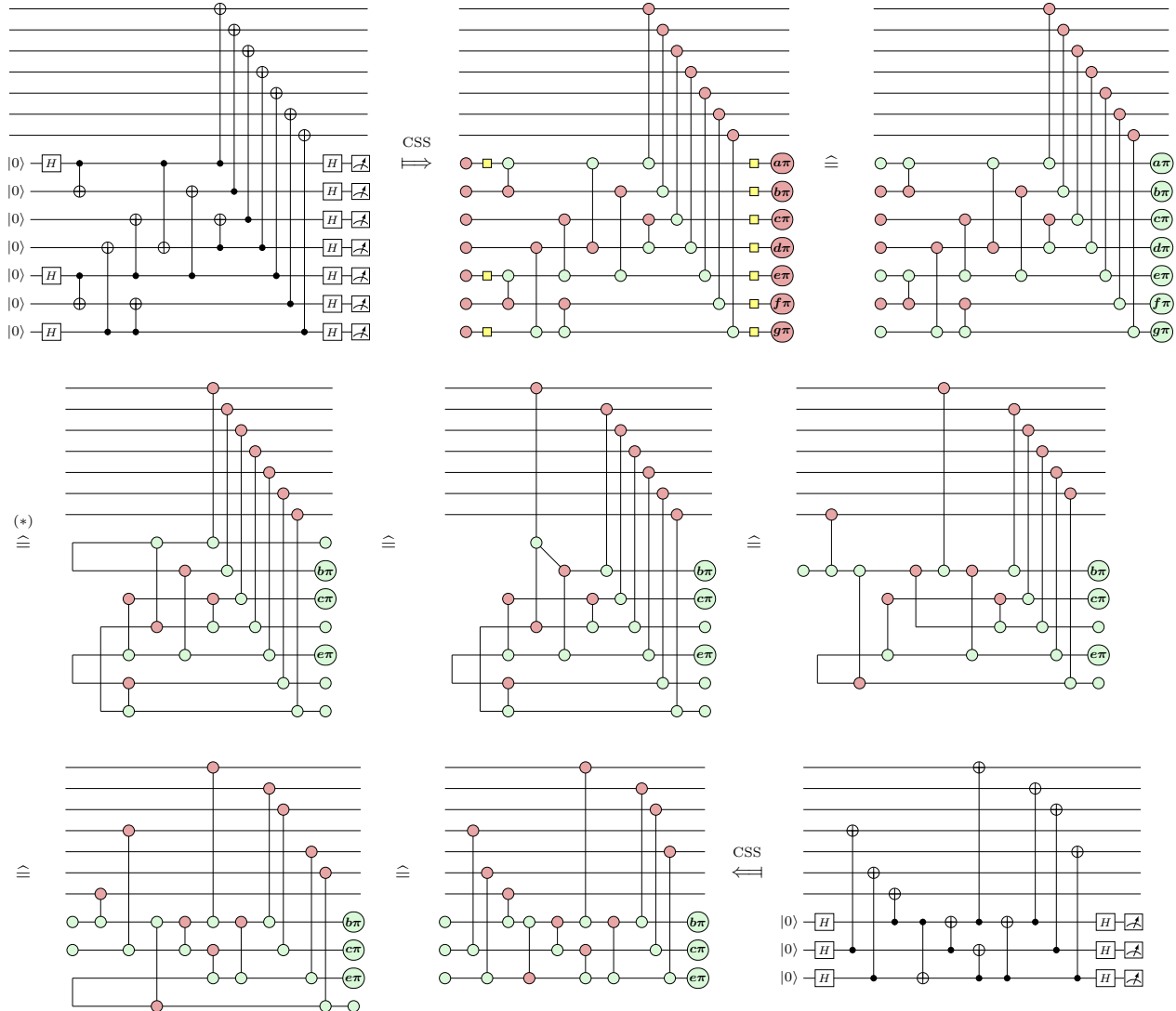
$$\text{rank}(H_x) = \text{rank} \begin{pmatrix} 1 & 1 & 1 & 1 & 0 & 0 & 0 \\ 0 & 1 & 1 & 0 & 1 & 1 & 0 \\ 0 & 0 & 1 & 1 & 0 & 1 & 1 \end{pmatrix} = 3 \quad \text{rank}(H'_x) = \text{rank} \begin{pmatrix} 1 & 1 & 0 \\ 1 & 1 & 1 \\ 0 & 1 & 0 \end{pmatrix} = 3$$

□

**Theorem 2.** The following transformation is fault-equivalent:



*Proof.* Same arguments as Theorem 2.



Note: While we only use fault-equivalent rewrites and show that the transformation is fault-equivalent, it is not necessary for this proof as it is already a non-FT implementation of the SE circuit.  $\square$

## Appendix B: Optimality of CNOT count

For the task of non-destructive syndrome measurement of the Steane code, we argue that our methods are optimal. First, we show that the non-FT circuit is optimal for CNOT count, and then argue that flagging such an implementation requires at least 3 CNOTs, making the FT version also optimal in CNOT count.

**Proposition 3.** For a non-destructive (and non-fault-tolerant) measurement of the three  $Z$ -syndromes of the Steane code, using three  $Z$  basis ancilla qubits and CNOT operations between data $\rightarrow$ ancilla and ancilla $\rightarrow$ ancilla, the minimal number of CNOT gates required is 11.

*Proof.* This problem can be understood as the construction of the parity-check matrix where only certain operations are allowed. Model the state of the ancilla qubits by a  $3 \times 7$  binary matrix  $M$  whose rows index ancillae  $a_0, a_1, a_2$  and columns index data qubits  $d_0, \dots, d_6$ . The initial matrix is the zero matrix and the target is the Steane parity-check matrix

$$H = \begin{pmatrix} 1 & 1 & 1 & 1 & 0 & 0 & 0 \\ 0 & 1 & 1 & 0 & 1 & 1 & 0 \\ 0 & 0 & 1 & 1 & 0 & 1 & 1 \end{pmatrix}.$$

Each allowed primitive operation counts for one CNOT:

- a  $data \rightarrow ancilla$  CNOT toggles a single entry  $M_{ij}$  (a single-entry flip);
- an  $ancilla \rightarrow ancilla$  CNOT adds one row to another ( $row_s \leftarrow row_s + row_r$ ).

*Proof by exhaustion (computer-assisted)* As the state space of  $3 \times 7$  binary matrices is finite ( $2^{21}$  states) and the allowed moves are simple, we can view the process as a finite unweighted directed graph whose vertices are  $3 \times 7$  binary matrices and whose edges correspond to the primitive operations. A breadth-first search (BFS) from the zero matrix visits vertices in order of increasing total number of primitive operations; the distance (graph shortest-path length) from the zero matrix to  $H$  is therefore the minimal number of CNOTs required in this setting.

We performed an exhaustive BFS from the zero matrix and found that no path of length  $\leq 10$  reaches  $H$ , while there exists a path of length 11, and indeed, Figure 2b is one such construction. Therefore, the graph distance is exactly 11, and therefore any protocol of the allowed type requires at least 11 CNOTs.

Implementation of the BFS can be found in [23] □

**Proposition 4.** Let  $C$  be any non-destructive, CNOT-only circuit that measures the three Steane  $Z$ -syndromes using three ancilla qubits  $a_0, a_1, a_2$  and exactly 11 CNOT gates. Then  $C$  must be augmented with at least three additional CNOT gates in order to flag (on a separate ancilla) every single-qubit ancilla fault that can propagate to the data as a weight-two  $Z$  error.

*Proof.* We give a computer-assisted exhaustive proof in the same style as the non-fault-tolerant optimality theorem. We consider all length-11 circuits that measure the three  $Z$ -syndromes using the allowed operations. For every such circuit  $C$ , in order to flag every single-ancilla  $Z$  fault that could propagate to a weight-two  $Z$  on the data, one must add at least three extra CNOT gates to the circuit. The proof proceeds by exhaustive enumeration and exact Pauli-propagation simulation.

*Proof by exhaustion (computer-assisted)* The search space of base circuits was exhaustively enumerated. For each base circuit  $C$ , the following steps were performed:

1. Simulate Pauli propagation to list all ancilla space-time locations at which an ancilla- $Z$  fault would propagate into a weight-two data  $Z$ , up to multiplication by stabilizers;
2. Search all sets of additional CNOTs that can flag any single fault identified in (1);
3. Record the minimal number  $m(C)$  of extra CNOTs required.

*Result of the exhaustive search* The exhaustive run found that, for every enumerated and valid length-11 circuit, the value  $m(C)$  satisfies  $m(C) \geq 3$ . In other words, with one or two additional CNOTs, no length-11 implementation can flag all ancilla- $Z$  faults that would otherwise propagate to weight-two data errors. Hence, to convert any such 11-CNOT implementation into one that flags all dangerous ancilla faults on a separate ancilla (i.e. so that each dangerous fault raises a flag), one must add at least three additional CNOT gates.

Implementation of the exhaustive search and a summary of the run can be found in [23] □